ISSN 0003-701X, Applied Solar Energy, 2016, Vol. 52, No. 1, pp. 1–4. © Allerton Press, Inc., 2016.
Original Russian Text © A.S. Saidov, K.A. Amonov, B.R. Kutlimurotov, 2016, published in Geliotekhnika, 2016, No. 1, pp. 3–7.

DIRECT CONVERSION OF SOLAR ENERGY TO ELECTRIC ENERGY

Direct Solar Conversion to Electricity Nanoscale Effects in pSi–$n(Si_2)_{1-x}(ZnSe)_x$ ($0 \le x \le 0.01$) of Solar Cells

A. S. Saidov[a], K. A. Amonov[a], and B. R. Kutlimurotov[b]

[a] *Physics and Technology Institute, Academy of Science, Republic of Uzbekistan, Tashkent*
[b] *Ion-Plasma and Laser Technology Institute, Academy of Science, Republic of Uzbekistan, Tashkent*
e-mail: amin@uzsci.net

Received October 12, 2015

Abstract—Epitaxial layers of the solid solutions $(Si_2)_{1-x}(ZnSe)_x$ ($0 \le x \le 0.01$) of n-type conductivity on pSi base were cultivated by liquid phase epitaxy from a restricted amount of tin solution–melt. The spectral photosensitivity dependence of the pSi–$n(Si_2)_{1-x}(ZnSe)_x$ structure was studied. A peak was discovered in the response level within the interval of photon energy from 2.67 to 3 eV conditioned by the energy band of ZnSe "quantum dots," which is located ~1.55 eV lower than the ceiling of the silicon valence band.

DOI: 10.3103/S0003701X16010102

The main factor to increase solar cell (SC) efficiency is a reduction of energy loss for high energy ($E_{h\nu} > E_g$) and low energy ($E_{h\nu} < E_g$) photons. Practical implementation of the extrinsic photovoltaic effect, which appeared upon the absorption of the high energy [1, 2] and low energy [3] photons, makes it possible to solve this problem. However, there is no currently available experimental data concerning implementation of the extrinsical photovoltaic effect based on the selection of the main semiconductor and corresponding photovoltaic interstitial diffusant.

This paper provides the results of an experimental survey of the multicomponent solid solution (SS) $(Si_2)_{1-x}(ZnSe)_x$ grown by the liquid-phase epitaxy method from a limited volume of the tin solution–melt based on the technology described in the paper [4]. Multicrystal plates Si of the p conductivity type with crystallographic orientation (111) were used as a base. The solution melt content was determined on the basis of preliminary experimental surveys of the liquid phase system Si–ZnSe–Sn and data taken from [5–7]. Cultivation of the layers was carried out by forced cooling in the atmosphere of palladium-purified hydrogen. The forced cooling rate at the optimum condition was 1–1.5 deg/min. Layer crystallization was carried out within the temperature interval of 950–750°C. The epitaxial layers had n-type conductivity and ~10 μm thickness.

Analysis of the chemical content of the surface and chips of cultivated samples made on an X-ray microanalyzer (Jeol, JSM 5910 LV-Japan) shows that the distribution of the components in the epitaxial layer $(Si_2)_{1-x}(ZnSe)_x$ changes within $x = 0$–0.0075.

Figure 1 shows the distribution profile of the components by the depth of the epitaxial layer. It is seen that the ZnSe content in the epitaxial layer increases nonmonotonously during cultivation of the solid solution $(Si_2)_{1-x}(ZnSe)_x$; this may be explained by the lack of oversaturation of the solution-melt in the liquid phase in relation to the ZnSe molecules. The ZnSe content then increases rapidly and achieves the value $x = 0.0075$ on the surface of the film. As the layer growth occurs within the restricted volume, the ZnSe concentration in the liquid phase gradually decreases, resulting in a gradual decrease of the ZnSe mole fraction in the solid phase.

The surface state of the cultivated epitaxial layers was studied with an atomic-force microscope at the Ion-Plasma and Laser Technology Institute, Academy of Science, Republic of Uzbekistan. Figures 2a and b show 2-D and 3-D views of the surfaces of the $(Si_2)_{1-x}(ZnSe)_x$ epitaxial films. It is seen that formation of island regions (nanocrystals) takes place from the components on the surface of the epitaxial layer (1–2 μm) in the growth process, i.e. the "quantum dots" are of the different sizes and heights (Fig. 2b). These nanocrystals, the so-called quantum dots, create a local electrostatic field at a distance of 25–75 nm; the field voltage is $E = 10^6$–10^8 V/cm, in accordance with the Keldysh-Franz effect [8]. In the semiconductor solid solutions $(Si_2)_{1-x}(ZnSe)_x$, the ZnSe monocrystal material increases during the growth process of those solutions. The X-ray structural analysis showed that subcrystallites of the ZnSe component with crystallographic orientation (220) and blocks of 63 nm widths were available in the crystal lattice of the solid solution [9]. Scanning of the surficial region of the film with the atomic-force microscope revealed island regions of the nanoinclusions with a height of 12 nm and width of 70 nm (Fig. 2). It seems that those inclusions correspond to the ZnSe subcrystallites that possess their

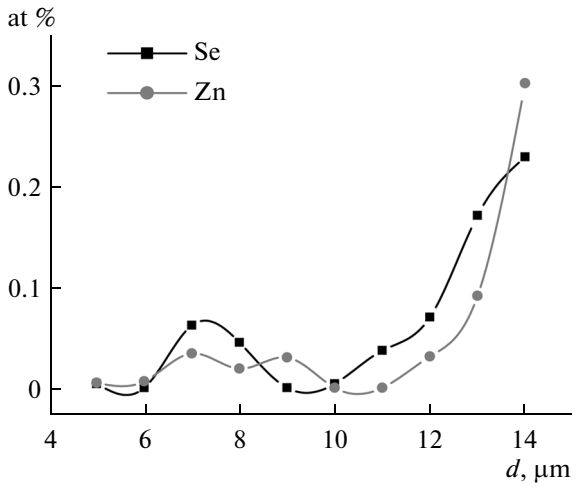

Fig. 1. Distribution profile of ZnSe in the epitaxial layer of the solid solution $(Si_2)_{1-x}(ZnSe)_x$

own energy spectrum, the gap width, and the lattice parameter (Fig. 3). In [10] it is shown that ZnSe is formed in the form of the nanocrystal. If the gap width of the nanocrystal is greater than that for the base semiconductor, then this nanocrystal will be a quantum dot; if the gap width of the nanocrystal is less than the base semiconductor, then a "quantum well" is formed.

Such a strong local electric field will lead to a change of the gap of the solid solution around the quantum dots, i.e., there is a unique opportunity to a form local, nanosized, variable-gap structure [11].

The spectral dependences of the photosensitivity of the pSi–$n(Si_2)_{1-x}(ZnSe)_x$ ($0 \le x \le 1$) structures were analyzed to reveal the ZnSe impact on the photosensitivity of the silicon patterns. Figure 4 shows the spectral dependence of the photosensitivity of the pSi–$n(Si_2)_{1-x}(ZnSe)_x$ ($0 \le x \le 1$) pattern at room temperature. It was measured by an optical spectrometer equipped with a specular monochromator (CARL ZEIS JENA) with quartz optics, which made it possible to analyze samples within a photon energy range of 1.1 to 3 eV. It is seen from Fig. 4 that if we change the emitted nSi layer of the solid solution $n(Si_2)_{1-x}(ZnSe)_x$ ($0 \le x \le 0.01$), then the spectral sensitivity of the silicon pSi-$n(Si_2)_{1-x}(ZnSe)_x$ patterns expands towards the short waves.

The maximum photosensitivity is found at a photon energy of 1.689 eV (Fig. 4); this may be explained by the width of the gap of the solar cell $n(Si_2)_{1-x}(ZnSe)_x$ ($0 \le x \le 1$). The decrease in photosensitivity at a photon energy of more than 1.7 eV is explained, in our opinion, by the burial depth of the separating barrier of the p–n transition, which is determined by the width of the epitaxial layer (which was ~10 μm in our case). The diffusion length of the minority current carriers in the $(Si_2)_{1-x}(ZnSe)_x$ ($0 \le x \le 1$) layer equals $L = 3.4$ μm, which is considerably less than the burial depth of the separating barrier.

A sensibility peak is clearly revealed on the photosensitivity spectrum of the analyzed structure within the photon energy interval from 2.6 to 3 eV (Fig. 4), which may be caused by the ZnSe wide zone component. It is known that the covalent bond of the ZnSe molecule atoms in the pure ZnSe semiconductor material, as expressed by $E_{g,ZnSe} = 2.70$ eV, will be stronger as compared to the Si–Si bond. However, it takes place when a ZnSe molecule displaces two silicon atoms in the tetrahedral silicon lattice (Fig. 3). It seems that this results in the formation of the impurity energy level of the ZnSe quantum dots located below the silicon valent zone ceiling by $\Delta E_i = E_{ph} - E_{g,\,s.s.} \approx 1.55$ eV (Fig. 5), where ZnSe quantum dots form the energy band in the silicon valent zone; the width of this zone is 0.3 eV [12]. Because the ZnSe is a direct band and Si–Si is not a direct band, its absorption

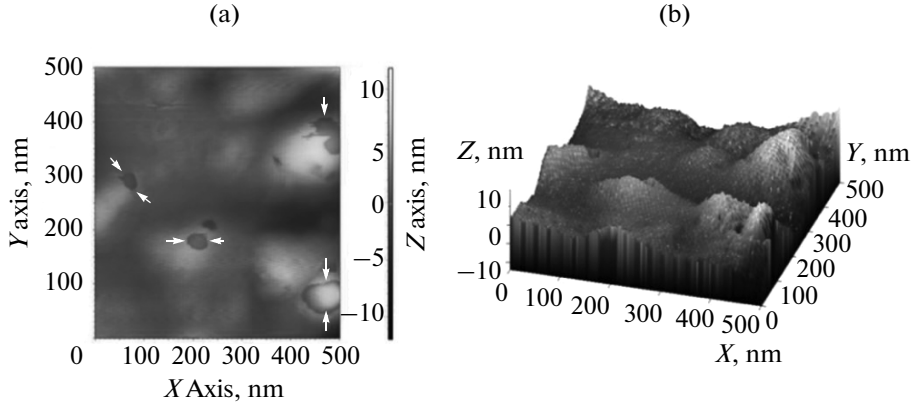

Fig. 2. Two-D (a) and 3-D (b) views of the surface of $(Si_2)_{1-x}(ZnSe)_x$, epitaxial films obtained with an atomic-force microscope. The image size is 500 × 500 nm^2, the height of the quantum dots is 5–15 nm, and the width is 25–78 nm.

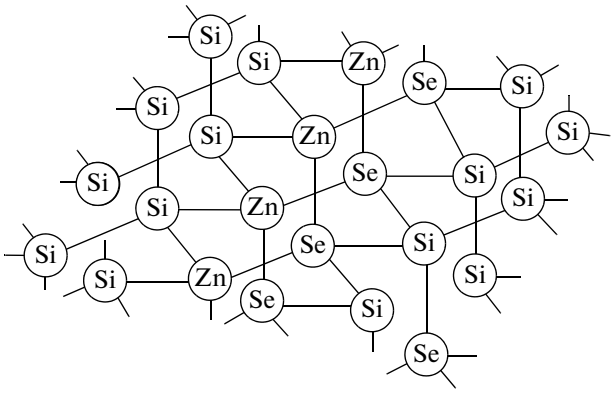

Fig. 3. Spatial configuration of the tetrahedral molecules bonds of the continuous solid substitutional solution $(Si_2)_{1-x}(ZnSe)_x$.

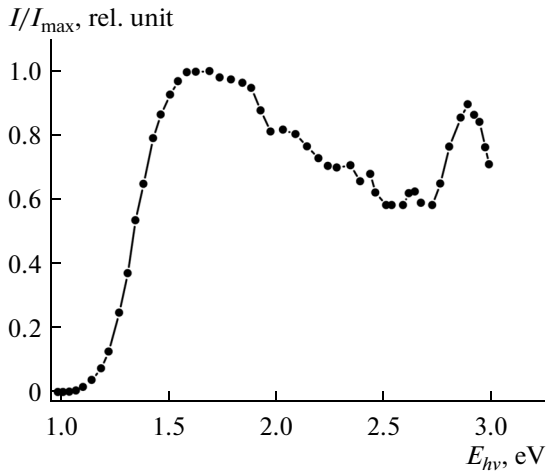

Fig. 4. Photosensitivity spectrum of the pSi–$n(Si_2)_{1-x}(ZnSe)_x$ $(0 \le x \le 0.01)$ patterns at room temperature.

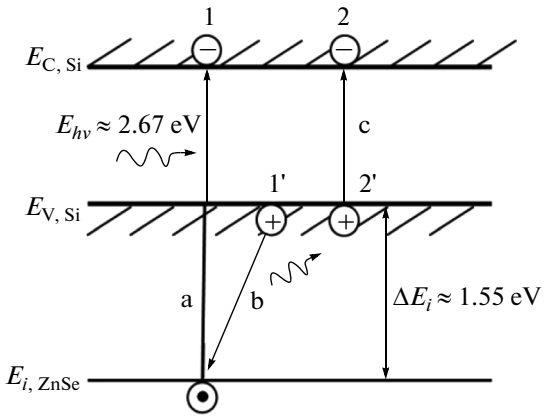

Fig. 5. Energy zone diagram of the $(Si)_{1-x}(ZnSe)_x$ $(0 \cong x \le 1)$ solid solution.

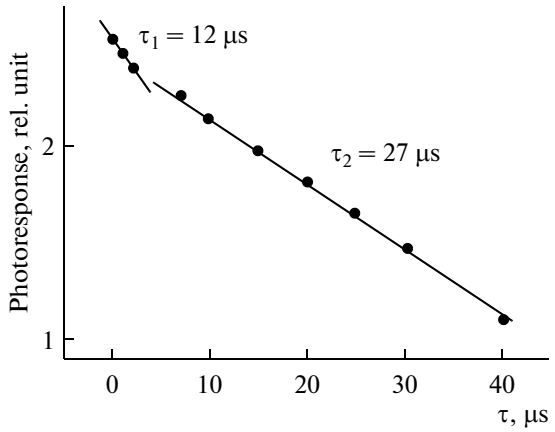

Fig. 6. Photorelaxation curves of the pSi–$n(Si_2)_{1-x}(ZnSe)_x$ $(0 \le x \le 0.01)$ structure.

coefficient in its absorption region is higher than that for the silicon absorption coefficient.

Therefore, the sectional area of electron photoemission with ZnSe impurity molecules is more than the sectional area of electron photoemission with Si–Si bond. X-ray microanalysis shows that the ZnSe mole content in the cultivated epitaxial layers is 1×10^{20} cm^{-3}; that is why samples with ZnSe impurities show an increased photo response in the spectrum short wave area. It seems that this is stipulated by the influence of the photo voltaic effect on the valent-zone ZnSe impurity; this effect means that quants with the $E_{ph} \ge 2E_{g,Si}$ energy absorbed by ZnSe impurities create wells located on the impurity levels (transition – a, Fig. 5), electrons may go over their places from the ceiling of the silicon of the valent zone emitting quants with the $h\nu \ge E_{g,Si}$ energy (transition Fig. 5, b). Those quants, being absorbed by the silicon atoms, create additional electron–hole pairs (transition Fig. 5, c). As a result, one photon with $E_{ph} \ge 2E_{g,Si}$ energy generates two pairs of the photon carriers (1,1' and 2,2'), according to the Nozick effect [13].

The relaxation time of the nonequilibrium carriers (τ) in the solid solution $(Si_2)_{1-x}(ZnSe)_x$ was evaluated on the basis of the photoconductivity relaxation of the nonequilibrium carriers at a low excitation level [14]. Excitation of the nonequilibrium carriers was carried out by laser emission with a wave length of $\lambda = 0.67$ μm in its absorption area.

The relaxation curve is described by the exponential dependence

$$\Delta n = \Delta n_o e^{-\frac{t}{\tau}}, \quad (1)$$

where Δn_0 is the concentration of nonequilibrium carriers upon photo excitation of the sample, Δn is the concentration of the nonequilibrium carriers within time t after removing excitation, and τ is the constant

time of relaxation. The constant time of relaxation was calculated on the basis of the slope angle of the exponential section of the $\ln(\Delta n) = \ln(\Delta n_0) - \frac{1}{\tau}t$ dependence. Figure 6 shows the relaxation curves for pSi–$n(Si_2)_{1-x}(ZnSe)_x$ in the semilog scale. It is seen from Figure 6 that the relaxation curve of the pattern has two sections with a constant relaxation time $\tau_1 \approx 12$ μs and $\tau_2 \approx 27$ μs, which supports the existence of mainly two types of effective recombination centers in the $(Si_2)_{1-x}(ZnSe)_x$ layer [15]. In such cases the effective relaxation time (τ_{ef}) of the nonequilibrium carriers is determined by the following equation:

$$\frac{1}{\tau_{ef}} = \frac{1}{\tau_1} + \frac{1}{\tau_2}. \quad (2)$$

The relaxation time of nonequilibrium carriers, as calculated by formula (2), was $\tau_{ef} \approx 8.3$ μs.

Thus, analysis of the spectra of pSi–$n(Si)_{1-x}(ZnSe)_x$ ($0 \le x \le 0.01$) heterostructure photosensitivity shows that SS $(Si)_{1-x}(ZnSe)_x$ ($0 \le x \le 0.01$) had the widest photosensitivity range at a photon energy of 1.1–3 eV, which was due to the ZnSe components in Si with differing ionization energy values of the covalent bond of the corresponding ZnSe molecules. The existence of impurity states in the zone diagram of the solid solution is confirmed by the formation of nanocrystals—quantum dots of the following size: the height is ~10 nm and width is ~70 nm. Such solid solutions may be used as photoactive material for solar cells operating within a wide spectrum range.

REFERENCES

1. Keevers, M.J. and Green, M.A., *Appl. Phys.*, 1994, vol. 75, no. 8, pp. 4022–4031.
2. Luque, A. and Marti, A., *Phys. Rev. Lett.*, 1997, vol. 78, no. 26, pp. 5014–5017.
3. Saidov, M.S., *Geliotekhnika*, 2002, no. 1, pp. 3–6.
4. Saidov, A.S., Razzakov, A.Sh., Risaeva, V.A., and Koschanov, E.A., *Mater. Chem. Phys.*, 2001, vol. 68, pp. 1–6.
5. Andreev, V.M., Dolginov, L.M., and Tret'yakov, D.N., *Zhidkostnaya epitaksiya v tekhnologii poluprovodnikovykh priborov* (Liquid Epitaxy in Semiconductor Devices), Moscow: Sov. Radio, 1975.
6. Hansen, M. and Anderko, K., *Constitution of Binary Alloys*, New York: McGraw-Hill, 1958.
7. Saidov, A.S., Saidov, M.S., and Koshchanov, E.A., *Zhidkostnaya epitaksiya kompensirovannykh sloev arsenida galliya i tverdykh rastvorov na ego osnove* (Liquid Epitaxy for Compensated Layers of GaAr and Solid Solutions on Its Based), Tashkent: Fan, 1986.
8. Fistul', V.I., *Vvedenie v fiziku poluprovodnikov: Ucheb. posobie dlya VUZov* (Introduction to Semiconductors Physics. Student's Book for High School), Moscow: Vysshaya Shkola, 1984.
9. Bakhadyrkhanov, M.K., Isamov, S.B., Iliev, Kh.M., et al., Silicon-based photocells of enhanced spectral sensitivity with nano-sized graded band gap structures, *Appl. Solar Energy*, 2014, vol. 50, no. 2, p. 61.
10. Saidov, A.S., Usmonov, Sh.N., and Saidov, M.S., Liquid-phase epitaxy of the $(Si_2)_{1-x-y}(Ge_2)_x(GaAs)_y$ substitutional solid solution ($0 \le x \le 0.91$, $0 \le y \le 0.94$) and their electrophysical properties, Semiconductors, 2015, vol. 49, no. 4, pp. 547–550.
11. Maronchuk, I.E., Kulyutkina, T.F., Maronchuk, I.I., and Bykovskii, S.Yu., Liquid-phase epytaxy and properties of nanoheterostructures based on III-V compounds, *Nanosist., Nanomater., Nanotekhnol.*, 2012, vol. 10, no. 1, pp. 77–88.
12. Farenburch, A.L. and Bube, R.H., *Fundamentals of Solar Cells: Photovoltaic Solar Energy Conversion,* London: Academic, 1983.
13. Saidov, A.S., Usmonov, Sh.N., Leyderman, A.Y., and Amonov, K.A., Influence of gamma-irradiation on photo-electric parameters of pSi–$n(Si_2)_{1-x}(ZnSe)_x$ structures, *Uzb. J. Phys.*, 2010, vol. 12, nos. 4–6, pp. 378–383.

Translated by E. Grishina